



Article

The Response of Denitrification to Increasing Water Temperature and Nitrate Availability: The Case of a Large Lowland River (Po River, Northern Italy) under a Climate Change Scenario

Maria Pia Gervasio , Giuseppe Castaldelli * and Elisa Soana

Department of Environmental and Prevention Sciences, University of Ferrara, Via Luigi Borsari 46, 44121 Ferrara, Italy; grvmrp@unife.it (M.P.G.); elisa.soana@unife.it (E.S.)

* Correspondence: ctg@unife.it

Abstract: Water warming and nutrient pulses following extreme rainfall events, both consequences of climate change, may have a profound impact on the biogeochemical dynamics of large temperate rivers, such as the Po River (Northern Italy), affecting denitrification capacity and the delivery of N loads to terminal water bodies. Manipulative experiments on denitrification kinetics were carried out using dark laboratory incubations of intact sediment cores collected from the lower Po River. Denitrification was measured along temperature and NO_3^- concentration gradients using ^{15}N additions, in summer and autumn, the two seasons when climate change-induced warming has been shown to be higher. The combination of increased temperatures and pulsed NO_3^- -enhanced denitrification, suggesting that electron acceptor availability limits the process. The direct link between climate change-induced effects and the positive response of denitrification may have implications for the improvement of water quality in the coastal zone, as it may help to partially buffer N export, especially in summer, when the risk of eutrophication is higher. Further research is needed to investigate the quality and quantity of sediment organic matter as important drivers regulating river denitrification.



Citation: Gervasio, M.P.; Castaldelli, G.; Soana, E. The Response of Denitrification to Increasing Water Temperature and Nitrate Availability: The Case of a Large Lowland River (Po River, Northern Italy) under a Climate Change Scenario.

Environments **2024**, *11*, 179.<https://doi.org/10.3390/environments11080179>

Academic Editors: Pengxiao Zhou, Qianqian Zhang, Fei Zhang and Zoe Li

Received: 3 July 2024

Revised: 7 August 2024

Accepted: 14 August 2024

Published: 20 August 2024



Copyright: © 2024 by the authors. Licensee MDPI, Basel, Switzerland. This article is an open access article distributed under the terms and conditions of the Creative Commons Attribution (CC BY) license (<https://creativecommons.org/licenses/by/4.0/>).

Keywords: climate change; nitrate pulses; temperature warming; denitrification; Po River

1. Introduction

As a result of human-induced climate change, extreme weather events are predicted to increase in frequency and intensity over the coming decades [1]. Precipitation and temperature anomalies are expected to alter both the magnitude and the timing of nutrient delivery from the watersheds to the coastal systems, as well as the biogeochemical dynamics of inland waters [2–4]. Intense rainfall generates large runoff and can mobilize and transport high amounts of nutrients, mostly as nitrate (NO_3^-) from agricultural fields, resulting in large pulses to aquatic ecosystems [5–7]. Rivers are highly dynamic ecosystems located at the interface between terrestrial and marine systems acting as nutrient filters and buffering the anthropogenic impacts on coastal zones. Through a variety of biogeochemical mechanisms, they determine the transformation, retention, or removal of nutrient loads before they reach the open sea [8–10]. Denitrification is considered to be a key anaerobic respiration leading to the permanent removal of bioavailable nitrogen (N) [11], and freshwater systems are estimated to account for about 20% of total global denitrification [12]. The process is carried out by a group of heterotrophic bacteria using NO_3^- as a terminal electron acceptor and reducing it to gaseous end-products (N_2 and N_2O) which diffuse into the atmosphere [13]. It occurs mainly in hypoxic-anoxic sediments and is supplied by NO_3^- diffusing from the water column or produced in the oxic layer by nitrification [14,15]. Water temperature and NO_3^- availability appear to be the main factors controlling denitrification, but little research has examined them together even though aquatic ecosystems, especially rivers, are increasingly subject to NO_3^- pulse inputs and are gradually warming [6,16,17].

The Po River is the largest river in Italy (Northern Italy) and the third Mediterranean river whose waters are subject to climate warming, especially in summer and fall [17]. The Po basin is one of the most intensively farmed and densely populated areas in Europe and a hot spot for NO_3^- pollution. In recent years, the effects of climate change have been observed in the basin, including an increase in the frequency of intense rainfall events with consequent sudden changes in runoff [18–20] and in the delivery and transformation of N loads. While short-term heavy precipitation events may dramatically increase the mobilization of NO_3^- , the progressive warming of the waters of the Po River may stimulate N dissipation processes and partially buffer the export of N to the coastal zones of the Adriatic Sea. These intertwined effects on the processing and transport of riverine N loads remain unexplored.

The aim of this work was to assess the combined effect of water temperature warming and NO_3^- pulse addition on N removal via denitrification in the Po River through controlled laboratory incubations of intact sediment cores. Summer and autumn were selected being the seasons when the effects of climate change are most evident in terms of temperature warming [18] and occurrence of extreme storm events [19,20]. In particular, the Po River water temperature has warmed over the last three decades, with the most pronounced signals in summer ($+0.13\text{ }^\circ\text{C yr}^{-1}$) and autumn ($+0.16\text{ }^\circ\text{C yr}^{-1}$), together with the strongest increase in the number of warm days ($+70\text{--}80\%$) [17].

2. Materials and Methods

2.1. Study Area and Sampling Procedure

The Po River is the biggest Italian river flowing, with an average discharge of $1500\text{ m}^3\text{ s}^{-1}$, from the Alps to the Adriatic Sea in Northern Italy (Figure 1) and has more than 140 tributaries and a capillary network of artificial canals [21]. The Po River basin is the largest cultivated area in Italy accounting for 35% of national agricultural production and the main source of nutrient inputs to the northern Adriatic Sea [22–24], making its coastal waters sensitive to eutrophication risk. The hydrological regime is characterized by two flood periods (spring and autumn) and two low-water periods (winter and summer). However, in recent decades, climate change affected this area with extreme events, such as the increase in heat wave frequency, the warming of water temperature, and the occurrence of prolonged drought periods [17,25]. In particular, the 2022 Po River hydrological drought was the worst in the last two centuries. The average daily discharge at the closing section was for more than three weeks below $168\text{ m}^3\text{ s}^{-1}$, i.e., the historical minimum recorded in the 1961–2021 period, and reached a new record of $104\text{ m}^3\text{ s}^{-1}$ on 24 July [25–27].

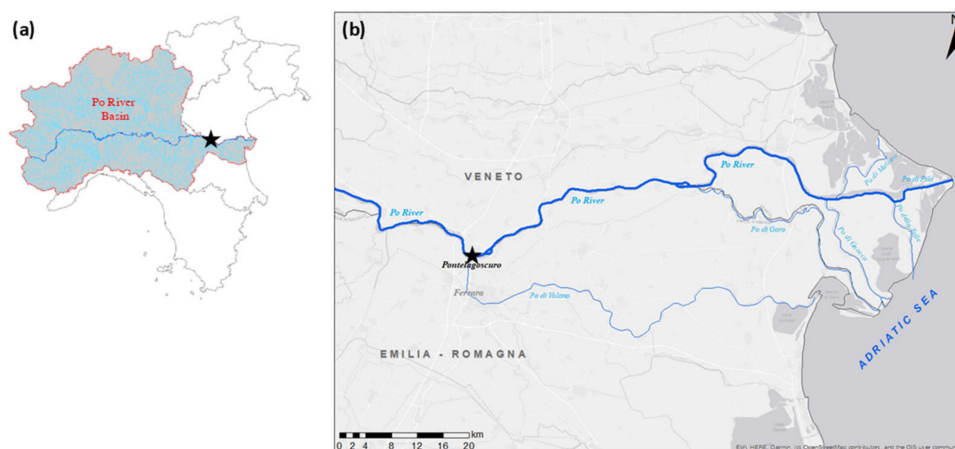


Figure 1. (a) Maps of the Po River Basin (red border), its main natural hydraulic network (light blue lines), and (b) of the sampling site (black star), i.e., the closing section at Pontelagoscuro (Ferrara province).

The study site was the closing section of the Po River basin, i.e., in the Pontelagoscuro locality (Ferrara province), right upstream of the deltaic system. Two sampling campaigns were carried out on 20 July and 15 November 2022, representative of summer and autumn conditions, respectively. In situ physicochemical parameters (temperature, oxygen concentration) were monitored using a multi-parameter probe (YSI 106 Model 85-Handheld Dissolved Oxygen, Conductivity, Salinity and Temperature System, Yellow Springs, OH, 107 USA), at the time of sediment sampling (Table 1).

Table 1. Water and sediment features at Pontelagoscuro site during the summer and autumn samplings. Standard deviations are reported in brackets.

Seasons	Temperature (°C)	O ₂ (mg L ⁻¹)	NO ₃ ⁻ (µM)	OM (%)	Density (g mL ⁻¹)	Porosity (%)
Summer	29	8.3	20 (2)	0.4 (0.03)	2.1 (0.1)	40 (3)
Autumn	14	10.2	135 (3)	1.7 (0.4)	1.8 (0.2)	60 (10)

In each season, 60 intact sediment cores (internal diameter 4.5 cm, length 20 cm) were sampled for the measurement of denitrification rates along the temperature gradient (15 cores were used for each of the 4 temperature treatments) and around 60 L of water were collected for core maintenance, pre- and incubation procedures. Additional cores (n = 5 for each season) were used for sediment characterization. Sediment samples were transported to the laboratory submerged in four tanks, corresponding to the four temperature treatments of each season, with site water continuously aerated using aquarium pumps. Each target temperature was set in the early afternoon of the day before incubation began to allow for acclimatization. The experimental temperatures were controlled in the incubation tanks by a thermostat and continuously monitored by a multi-parameter probe.

The experimental temperatures were controlled in the incubation tanks by a thermostat and continuously monitored using a multi-parameter probe [28]. Four different temperature treatments were applied in each seasonal incubation, i.e., 21, 25, 28, and 32 °C in summer and 9, 12, 16, and 20 °C in autumn. These threshold values were established based on historical temperature data for the Po River in the last three decades [17; 18; 28] and future predictions in the period of 2041–2070 [29]. The year 2022 was characterized by strong temperature anomalies. The water temperature of the Po River was constantly higher than the monthly mean values of the 2000–2021 period, with an average positive anomaly of 2.5 °C throughout the summer and until mid-autumn [18; 27].

2.2. Measurement of Benthic Oxygen Fluxes along Temperature Gradients

Benthic oxygen flux (sediment oxygen demand, SOD) was measured according to standardized protocols [30,31]. A Teflon-coated magnet driven by an external motor (40 rpm) was inserted into each core and suspended a few centimeters above the sediment–water interface to gently mix the water column. Sediments were incubated in the dark to simulate in situ conditions where the turbidity limits the light penetration to the benthic compartment [32]. Before incubation started, the water in the tanks was replaced with fresh water to maintain dissolved nutrient concentrations close to those found in the field. The water level in the tanks was lowered to a few centimeters below the top of the cores. Oxygen concentration was measured inside each core using a multi-parameter probe and each liner was then sealed with a gas-tight Plexiglass lid. Incubation lasted from 2 (summer experiment) to 4 h (autumn experiment), and at the end of the incubation period, the O₂ concentration in each core was measured again. These durations have been established on the basis of pilot tests as the minimum time required to detect significant changes in solute concentrations and to keep O₂ concentrations at the end of the incubation within 20% of the initial value, according to standard protocols [30].

The dark flux of O₂ (sediment oxygen demand, SOD; $\mu\text{mol O}_2 \text{ m}^{-2} \text{ h}^{-1}$) was calculated according to the following equation [31]:

$$\text{SOD} = \frac{|([\text{O}_2]_f - [\text{O}_2]_i)| \times V}{A \times t} \quad (1)$$

where the brackets indicate the O₂ concentration (μM) at the end (f) and at the beginning (i) of the incubation; V (L) is the water column volume; A (m^2) is the sediment surface; and t (h) is the incubation time.

2.3. Measurement of Denitrification along Temperature and NO₃[−] Gradients

After the SOD measurement, the water in the tanks was replaced with fresh water, and the intact cores were re-submerged for around 2 h to stabilize before the following incubation. The Isotope Pairing Technique (IPT; [33]) was applied to measure denitrification rates under increasing NO₃[−] concentrations at the four temperature treatments tested in each season. The water level in the tanks was lowered to a few centimeters below the top of the cores to isolate them. To obtain final ¹⁵NO₃[−] concentrations of 50, 100, 150, 200, and 250 μM , variable amounts of labeled NO₃[−] (20 mM Na¹⁵NO₃ stock solution, 98%, Sigma Aldrich, Inc. St. Louis, MO, USA) were added to the water phase of three replicates for each NO₃[−] level. To simulate extreme storm events, which have become more frequent in the Po basin in recent decades, an enrichment of almost 40% of the in situ NO₃[−] concentration was established [34,35].

To calculate the ¹⁵N- enrichment of the NO₃[−] pool, a water sample was collected from each core before and after (5 min) the labeled NO₃[−] addition. Water samples were collected from each core using a 60 mL glass syringe, filtered through Whatman GF/F glass fiber filters (pore size of 0.45 μm), transferred to 20 mL polyethylene scintillation vials, and analyzed with a Technicon AutoAnalyser II using the cadmium reduction method (detection limit of 0.4 μM ; [36]). After the water sampling, the cores were capped with gas-tight Plexiglass lids and incubated in the dark for 2 h and 4 h during the summer and autumn experiments, respectively. The incubations were set to ensure the O₂ consumption was less than 20% of the initial concentration, a requirement for IPT application [33]. At the end of the incubation, the sediment and water phases of each core were mixed to homogenize the dissolved N₂ pools in the aqueous phase and pore water. An aliquot of the slurry was transferred to glass-tight vials (12 mL, Exetainer[®], Labco Limited, Lampeter, UK) and fixed with 200 μL of ZnCl₂ (7 M) to stop microbial activity. The slurry samples were analyzed by Membrane Inlet Mass Spectrometry (MIMS; Bay Instruments, Easton, MD, USA; [37]) to determine the abundance of ²⁹N₂ and ³⁰N₂. The IPT is one of the most widely used techniques for the measurement of denitrification in aquatic ecosystems [38–40]. The measured production of ²⁹N₂ (p29) and ³⁰N₂ (p30) was used to calculate the denitrification rates ($\mu\text{mol N m}^{-2} \text{ h}^{-1}$) according to principles and equations reported by Nielsen [33] and reviewed by Steingruber et al. [39]. The denitrification of labeled ¹⁵NO₃[−] (D₁₅) was calculated from p29 and p30, as follows:

$$D_{15} = p29 + 2 \times p30 \quad (2)$$

Assuming a binomial distribution of ²⁸N₂, ²⁹N₂ and ³⁰N₂, Nielsen ([33]) derived the following equations for the calculation of denitrification of unlabeled ¹⁴NO₃[−] (D₁₄) and of total denitrification (D_{tot}):

$$D_{14} = D_{15} \times \frac{p29}{2 \times p30} \quad (3)$$

$$D_{\text{tot}} = D_{14} + D_{15} \quad (4)$$

Denitrification of the $^{14}\text{NO}_3^- / ^{15}\text{NO}_3^-$ mixture diffusing from the water column into the sediment (D_w^{tot}) was calculated as follows:

$$D_w^{\text{tot}} = \frac{D_{15}}{\varepsilon} \quad (5)$$

where ε is the isotopic NO_3^- enrichment, calculated as:

$$\varepsilon = \frac{[\text{NO}_3^-]_a - [\text{NO}_3^-]_b}{[\text{NO}_3^-]_a} \quad (6)$$

In Equation (6), the brackets indicate concentrations (μM), and the subscripts a and b refer to after and before the $^{15}\text{NO}_3^-$ tracer addition, respectively.

Denitrification of NO_3^- produced within the sediment by nitrification, i.e., coupled nitrification-denitrification (D_n), was obtained by difference:

$$D_n = D_{\text{tot}} - D_w^{\text{tot}} \quad (7)$$

Under the assumption that D_w^{tot} follows a linear increase with higher $^{15}\text{NO}_3^-$ tracer concentrations, the rate can be extrapolated back to tracer-free conditions in order to obtain the denitrification rate (D_w) of ambient nitrate ($^{14}\text{NO}_3^-$) diffusing from the water column to the sediment:

$$D_w = D_w^{\text{tot}} \cdot (1 - \varepsilon) \quad (8)$$

2.4. Sediment Characterization

The additional sediment cores were used to determine sediment features at each seasonal sampling. The upper 0–1 cm sediment layer was extracted, homogenized, and analyzed for bulk density (g mL^{-1}), measured as the weight of a known volume of fresh aliquot (5 mL), and porosity (%) after oven drying at 50°C for 72 h. Powered aliquots of the dried sediment were transferred to a muffle furnace at 350°C for 3 h to determine the organic matter content (OM, %) as loss on ignition.

2.5. Statistical Analysis

Linear regression was applied to determine the relation between water temperature and SOD and between $^{15}\text{NO}_3^-$ and D_{15} , using the software SigmaPlot 15.0 (Systat Software, Inc., San Jose, CA, USA). Denitrification rates of $^{15}\text{NO}_3^-$ were analyzed using linear mixed-effect (LME) models to detect differences in applied temperature [28] and NO_3^- level in each seasonal experiment. In the LME test, a random effect was applied to consider all replicate samples at each temperature and nitrate gradient. The sample size was equal in all tests. The LME test was run in rStudio (rStudio-2023.06.0-421) using the nlme package [41]. The focus of the test was to compare the differences in process rates at different temperatures and $^{15}\text{NO}_3^-$ concentrations and the correlation between the two factors by considering the season as a fixed factor. For all tests, the overall significance level was set at $p \leq 0.05$.

The response of D_w^{tot} to increasing NO_3^- concentrations was fitted to a linear model or a non-linear model representing an exponential curve or the Michaelis–Menten kinetic [42]:

$$D_w^{\text{tot}} = \frac{D_w^{\text{tot max}} \cdot [\text{NO}_3^-]}{K_m + [\text{NO}_3^-]} \quad (9)$$

where $D_w^{\text{tot max}}$ ($\mu\text{mol N m}^{-2} \text{h}^{-1}$) is the maximum denitrification rate, $[\text{NO}_3^-]$ is the sum of ambient $^{14}\text{NO}_3^-$ and added $^{15}\text{NO}_3^-$ (μM), and K_m is the Michaelis–Menten or half-saturation constant (i.e., the NO_3^- concentration at which $D_w^{\text{tot}} = 1/2 D_w^{\text{tot max}}$).

3. Results and Discussion

3.1. River Sediment Oxygen Demand along Seasonal Temperature Gradients

Water temperature warming significantly affected the benthic metabolism of the Po River, mainly by stimulating oxygen consumption because of increased respiration activity at higher temperatures, which agrees with previous outcomes in freshwater sediments [7,43,44]. In situ O_2 concentrations were different in summer and autumn sampling, with higher values in autumn than in summer (8.3 and 10.2 $mg\ L^{-1}$, respectively; Table 1), reflecting differences in gas solubility in relation to water temperature. The water of the Po River is well mixed in the section studied and along the whole of its upstream course, due to the high energy of the flow and its tortuous course. In fact, the O_2 concentrations measured at the time of sediment sampling, as in other seasons [18], were close to 100% saturation. Along the experimental temperature gradients, the SOD ranged between 56 ± 7 and 813 ± 149 $\mu mol\ O_2\ m^{-2}\ h^{-1}$ and between 926 ± 141 and 1584 ± 337 $\mu mol\ O_2\ m^{-2}\ h^{-1}$ in autumn and summer, respectively. In both seasons, the sediment oxygen demand followed a linear trend with temperature ($p < 0.05$ in summer, $p < 0.001$ in autumn; Figure 2), with a rise of ~ 55 and ~ 69 $\mu mol\ O_2\ m^{-2}\ h^{-1}$ for an increase of one degree of temperature in summer and autumn, respectively, highlighting a temperature dependence for microbial respiration [45].

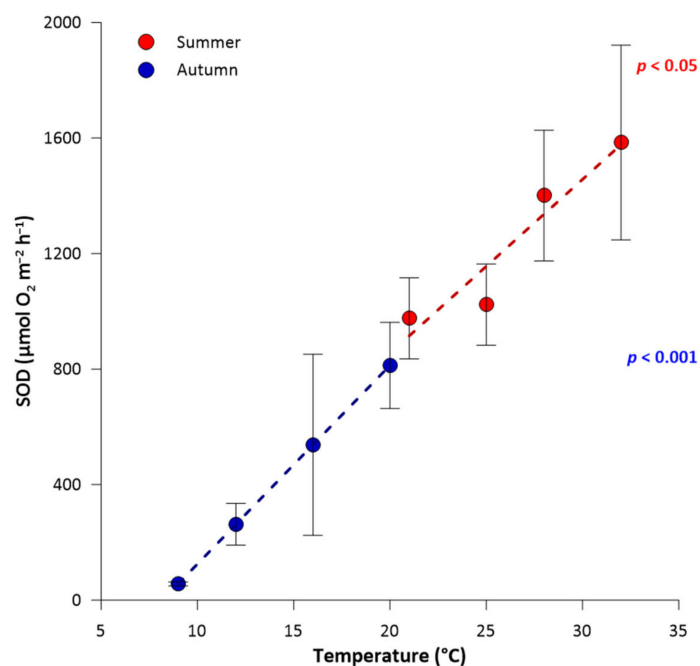


Figure 2. Sediment oxygen demand (SOD; $\mu mol\ O_2\ m^{-2}\ h^{-1}$) measured along the water temperature gradients. Average values \pm standard deviations are reported ($n = 15$). The dashed lines show the statistically significant trends indicated on the right.

3.2. Influence of Water Temperature and NO_3^- Concentration on Partitioning between D_w and D_n

Denitrification rates increased significantly along the experimental temperature gradients set in the two seasons, with the magnitude and partitioning between D_w and D_n strongly determined by NO_3^- availability in the water column (Figure 3), similar to the previous results for the Po River sediments [28]. Summer denitrification rates measured at in situ NO_3^- concentration ranged between 15 ± 7 $\mu mol\ N\ m^{-2}\ h^{-1}$ (at 21 °C) and 49 ± 7 $\mu mol\ N\ m^{-2}\ h^{-1}$ (at 32 °C), with D_w contributing to a minor fraction of the overall rate (18–38%) due to low NO_3^- availability in water (~ 20 μM). In contrast, higher water NO_3^- concentrations in autumn (~ 135 μM) resulted in a dominance of D_w (77–95%) to total denitrification rates, which varied between 9 ± 4 $\mu mol\ N\ m^{-2}\ h^{-1}$ (at 9 °C) and 65 ± 12 $\mu mol\ N\ m^{-2}\ h^{-1}$ (at 20 °C). D_n showed a positive response along the temperature

gradient in summer, varying from 10 ± 7 to $40 \pm 7 \mu\text{mol N m}^{-2} \text{h}^{-1}$ and accounting for 62–82% of the total rates, while D_w did not exhibit the same upward trajectory and remained below $10 \mu\text{mol N m}^{-2} \text{h}^{-1}$ across the whole temperature gradient. In contrast, in the autumn experiment, D_w was systematically higher than D_n , increasing 7-fold with an 11°C warming of water temperature.

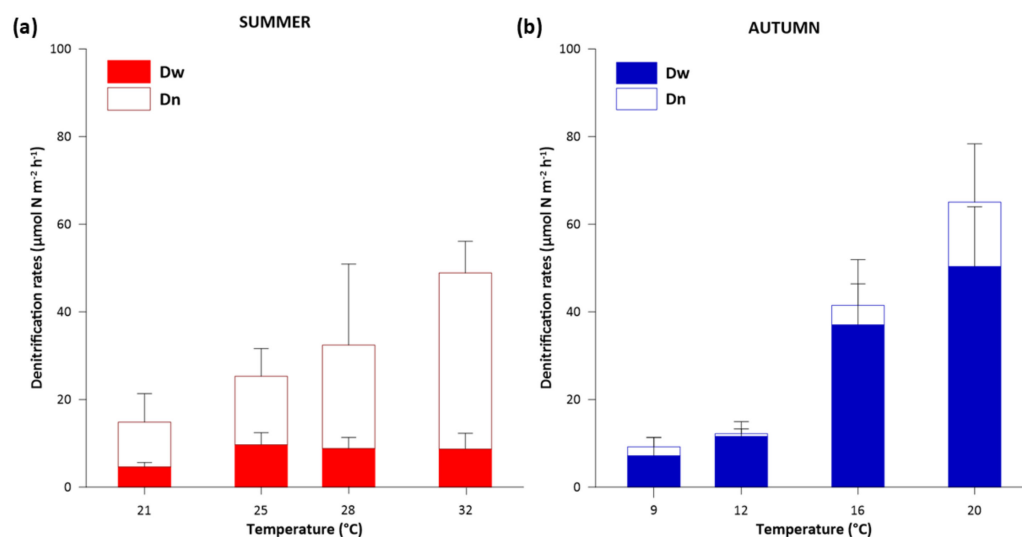


Figure 3. Denitrification rates measured along the temperature gradients in (a) summer and (b) autumn at ambient NO_3^- concentrations. Rates are split in the contribution of D_w (denitrification of water column NO_3^-) and D_n (denitrification of NO_3^- produced by nitrification in the oxic sediment layer). Average values \pm standard deviations ($n = 15$) are reported.

The positive effect of temperature on denitrification is well known for various aquatic ecosystems, including riverbed sediments [46,47]. The biological reaction rate generally increases by two or three times for each 10°C increase in temperature, as was also found in the present work. Water warming affects N removal via denitrification both as a direct effect on enzyme activity and as an indirect effect on sediment redox conditions [14,48,49]. Thus, higher water temperatures may reduce both O_2 solubility and increase sedimentary O_2 consumption, limiting O_2 penetration and extending the hypoxic-anoxic layer suitable for denitrifying bacteria [43,50]. As temperature increases, microbial activity accelerates consuming all available O_2 , resulting in the use of other electron acceptors to degrade organic matter [11,14]. The warming of the water increased sediment respiration and anaerobic processes and this, together with high NO_3^- concentrations in the water column, played an important role in enhancing denitrification, specifically favoring the prevalence of D_w over D_n . Increasing temperature may have also triggered the enzyme kinetics of nitrifying bacteria. The ammonia required for this process is derived from the mineralization of organic N, which is stimulated at higher temperatures [15,51].

3.3. Climate Change-Related Factors Controlling Denitrification

A collective study of several aquatic ecosystems confirmed the importance of temperature in controlling denitrification, but several other environmental factors have been shown to modulate its seasonal patterns [8]. Many studies have investigated the drivers of denitrification in isolation by manipulating temperature, NO_3^- , organic carbon, and other temperature-sensitive variables in laboratory assays [13]. However, climate change is expected to simultaneously alter several environmental factors that regulate denitrification. This highlights the need for studies that examine the effects of multiple controls, especially in large eutrophic rivers subject to extreme weather events.

The results of the present experiment showed that the combination of warmer temperatures and increased NO_3^- availability enhanced denitrification rates demonstrating

that the process was not saturated along the $^{15}\text{NO}_3^-$ gradient. Rates of $^{15}\text{NO}_3^-$ consumption measured in summer (Figure 4a) ranged between 15 ± 5 ($50 \mu\text{M}$, 21°C) and $125 \pm 20 \mu\text{mol N m}^{-2} \text{h}^{-1}$ ($250 \mu\text{M}$, 32°C). Summer rates were generally higher than the autumn rates (Figure 4b) measured along the same NO_3^- gradient but at lower temperatures. Indeed, D_{15} measured in autumn varied from 4 ± 3 ($50 \mu\text{M}$, 14°C) to $74 \pm 7 \mu\text{mol N m}^{-2} \text{h}^{-1}$ ($250 \mu\text{M}$, 20°C). The response of D_{15} to increasing labeled $^{15}\text{NO}_3^-$ concentrations followed a linear relation for all the temperature treatments tested in summer. It can be inferred that in lowland river stretches, during summer and autumn, denitrification may be constrained by the availability of electron acceptors. The sole exception to this trend was the highest temperature (32°C) when the pattern along the NO_3^- gradient was more erratic despite the highest rates being measured at the maximum NO_3^- concentration ($250 \mu\text{M}$) (Figure 4). The addition of $^{15}\text{NO}_3^-$ also stimulated D_{15} in autumn; in fact, the reduction rates increased linearly along the $^{15}\text{NO}_3^-$ gradient for all temperatures, except at the lowest one (9°C), confirming a microbial limitation at colder temperatures [52,53]. A breakpoint in the temperature response of denitrification may occur, reflecting the fact that rates decrease non-linearly at lower temperatures [11,54]. The LME statistical test (Table 2) showed the dependence of D_{15} from both temperature ($p < 0.001$) and NO_3^- availability in the Po River ($p < 0.001$), both in summer and in autumn. Moreover, there was a significant interaction between NO_3^- treatment and temperature, suggesting that the effect of substrate availability on denitrification was dependent on temperature as a key regulator of the enzymatic activity and of redox conditions [13,48].

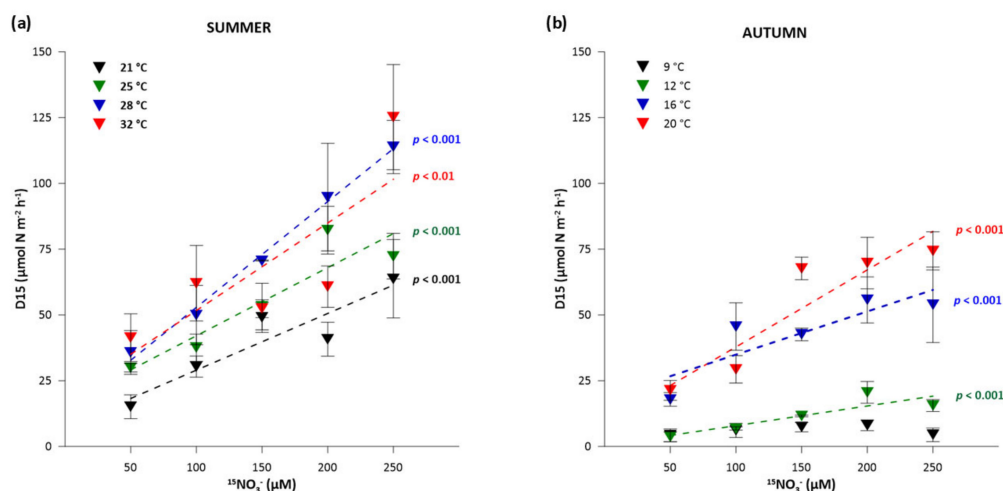


Figure 4. Denitrification rates of the $^{15}\text{NO}_3^-$ ($\mu\text{mol N m}^{-2} \text{h}^{-1}$) measured along the labelled NO_3^- concentrations (μM) gradient in (a) summer and in (b) autumn at the different seasonal temperatures. Average values \pm standard deviations ($n = 3$) are reported. The dashed lines show the statistically significant trend indicated on the right of the fitted curve.

Table 2. Effect of the factors (temperature and concentration of added $^{15}\text{NO}_3^-$) and their interaction on denitrification of labeled tracer (D_{15}) in summer and autumn, based on linear mixed effects (LME) models. F test value and significance level (p) are reported.

Season	Temperature ($^\circ\text{C}$)		$^{15}\text{NO}_3^-$ (μM)		Temperature \times $^{15}\text{NO}_3^-$	
	F	p	F	p	F	p
Summer	33.0	<0.001	115.7	<0.001	3.6	0.05
Autumn	202.3	<0.001	51.6	<0.001	32.6	<0.001

The lowest temperature treatment tested in summer (21 °C) was only one degree different from the highest temperature tested in autumn (20 °C). However, in autumn D_{15} rates were slightly higher, on average, under non-limiting NO_3^- concentrations (250 μM) (Figure 4). This underlines that other factors affecting denitrification may have varied seasonally. Sediment organic matter was more available in autumn (Table 1), which may have promoted denitrification. Sediment organic matter stimulates the process directly by providing substrate (i.e., electron donors) to heterotrophic denitrifiers, and indirectly by increasing O_2 consumption, reducing the thickness of the oxic zone [11].

In autumn, over the whole temperature gradient, the response of $D_{\text{W}}^{\text{tot}}$ (i.e., denitrification of the $^{14}\text{NO}_3^-/^{15}\text{NO}_3^-$ mixture diffusing from the water column into the sediment) to total NO_3^- availability (ambient $^{14}\text{NO}_3^-$ + added $^{15}\text{NO}_3^-$) showed asymptotic rates. This indicates the saturation of denitrification capacity, as shown by Michaelis–Menten curves (Figure 5). The kinetics of denitrification at high NO_3^- concentrations are quite uncertain, where either electron acceptor saturation or limitation by other controlling factors may occur [8,13], such as organic matter in sandy sediments of the Po River (Table 1). At the lower summer temperature (21 and 25 °C), a saturation over 220 μM was observed, while the increase in denitrification was exponential at the highest temperatures (28 and 32 °C). With increased electron acceptor availability, denitrification is released from substrate limitation, potentially allowing a greater response to temperature increase. The linear positive response may also be due to increased mineralization rates. This would release organic compounds and create a temperature-induced O_2 deficiency, which in turn may reduce the width of the oxic layer, resulting in a thinner diffusion path length for NO_3^- [14,43].

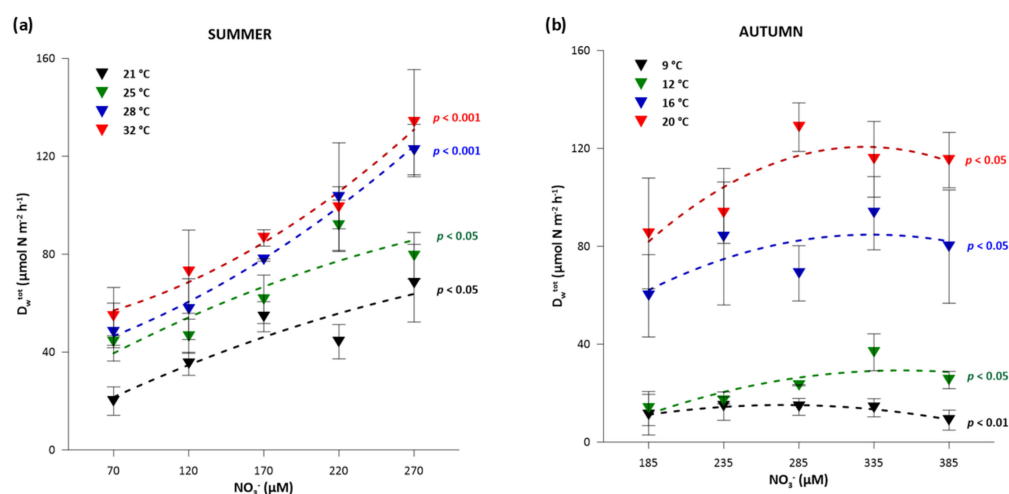


Figure 5. Denitrification of the $^{14}\text{NO}_3^-/^{15}\text{NO}_3^-$ mixture diffusing from the water column into the sediment ($D_{\text{W}}^{\text{tot}}$, $\mu\text{mol N m}^{-2} \text{h}^{-1}$) as a function of NO_3^- concentration (ambient $^{14}\text{NO}_3^-$ + added $^{15}\text{NO}_3^-$) in (a) summer and in (b) autumn at the different tested temperatures. Average values \pm standard deviations ($n = 3$) are reported. The dashed lines show the statistically significant trend indicated on the right of the fitted curve.

The observed denitrification rates compare well to those previously reported for several aquatic ecosystems of the Po River Basin [27]. Pulse NO_3^- additions resulted in an immediate stimulation of denitrification rates in the Po River sediments suggesting that the denitrification potential was only partially expressed. These results are consistent with other studies describing the dependence of denitrification on NO_3^- availability in freshwater sediments [55,56], as well as its control by other factors, such as organic matter content in sediments [43,57–61].

In the context of climate change, the sensitivity of denitrification to NO_3^- concentrations has important effects on water quality. The river self-depuration capacity supported by sediment denitrification appeared to be highly responsive to both temperature and

NO_3^- availability with implications for water quality improvement in the Adriatic Sea, due to the potential reduction in N loads especially when riverine nutrients trigger the most eutrophication.

4. Conclusions

Manipulative laboratory experiments demonstrated that water warming and pulse NO_3^- addition resulted in a stimulation of denitrification leading to permanent N removal in the Po River sediments. The direct link between climate-induced water temperature increase and the positive response of denitrification may have implications for the improvement of water quality in the Adriatic Sea, as it may contribute to partially buffer N loads, especially in summer when the eutrophication risk is higher. Challenges remain in scaling up NO_3^- removal via denitrification from sediment cores to ecosystems, and future studies are needed to explore the natural heterogeneity influencing the spatial and temporal variation of N cycling in river sediments. Interactions among NO_3^- availability, temperature, organic carbon, and discharge are important to consider when assessing the changes in river self-depuration capacity under future climate scenarios. Exploring these might provide a more nuanced understanding of the river's response to environmental changes. The efficiency of rivers as nutrient filters depends on factors other than the kinetics of denitrifiers, such as water residence time, which decreases during high-flow events. Finally, comprehensive experiments should be planned to fully understand the role of carbon limitation in controlling nitrous oxide production via incomplete denitrification.

Author Contributions: Conceptualization, M.P.G., G.C. and E.S.; methodology, E.S. and G.C.; investigation, M.P.G., E.S. and G.C.; formal analysis, M.P.G.; writing—original draft preparation, M.P.G. and E.S.; writing—review and editing, G.C.; visualization, M.P.G.; funding acquisition, G.C.; supervision, G.C. and E.S. All authors have read and agreed to the published version of the manuscript.

Funding: This study was financially supported by the Consorzio di Bonifica Pianura di Ferrara (Ferrara Plain Reclamation Consortium) as part of a long-term collaboration aimed at defining management strategies to control eutrophication in the Po Delta region. This research was also funded by the Emilia-Romagna Region, in the framework of the project “Assessment and mapping of the productivity of the bivalve mollusc aquaculture in the Sacca di Goro lagoon and the coastal stretch from Lido di Volano to Lido delle Nazioni, Ferrara, Emilia-Romagna” (Hunting and Fisheries Division) and by the EcosistER Project, under the National Recovery and Resilience Plan (NRRP), within WP3—Biotic and abiotic marine resources of the Spoke 5—Circular economy and blue economy.

Data Availability Statement: The raw data supporting the conclusions of this article will be made available by the authors upon request.

Acknowledgments: The authors are grateful to Anna Gavioli (University of Ferrara) for her valuable advice on statistics and to Fabio Vincenzi (University of Ferrara) for his help with sampling.

Conflicts of Interest: The authors declare no conflicts of interest.

References

1. IPCC. *IPCC, 2021: Climate Change 2021: The Physical Science Basis. Contribution of Working Group I to the Sixth Assessment Report of the Intergovernmental Panel on Climate Change*; Cambridge University Press: Cambridge, UK, 2021.
2. Whitehead, P.G.; Wilby, R.L.; Battarbee, R.W.; Kernan, M.; Wade, A.J. A Review of the Potential Impacts of Climate Change on Surface Water Quality. *Hydrol. Sci. J.* **2009**, *54*, 101–123. [[CrossRef](#)]
3. Zhao, G.; Merder, J.; Ballard, T.C.; Michalak, A.M. Warming May Offset Impact of Precipitation Changes on Riverine Nitrogen Loading. *Proc. Natl. Acad. Sci. USA* **2023**, *120*, e2220616120. [[CrossRef](#)] [[PubMed](#)]
4. Liu, S.; Hu, K.; Xie, Z.; Wang, Y. Seasonal Constraint of Dynamic Water Temperature on Riverine Dissolved Inorganic Nitrogen Transport in Land Surface Modeling. *Atmos. Ocean. Sci. Lett.* **2024**, *17*, 100485. [[CrossRef](#)]
5. Gao, Y.; Zhu, B.; Yu, G.; Chen, W.; He, N.; Wang, T.; Miao, C. Coupled Effects of Biogeochemical and Hydrological Processes on C, N, and P Export during Extreme Rainfall Events in a Purple Soil Watershed in Southwestern China. *J. Hydrol.* **2014**, *511*, 692–702. [[CrossRef](#)]
6. Ballard, T.C.; Sinha, E.; Michalak, A.M. Long-Term Changes in Precipitation and Temperature Have Already Impacted Nitrogen Loading. *Environ. Sci. Technol.* **2019**, *53*, 5080–5090. [[CrossRef](#)]

7. Van Vliet, M.T.H.; Thorslund, J.; Stokal, M.; Hofstra, N.; Flörke, M.; Ehalt Macedo, H.; Nkwasa, A.; Tang, T.; Kaushal, S.S.; Kumar, R.; et al. Global River Water Quality under Climate Change and Hydroclimatic Extremes. *Nat. Rev. Earth Environ.* **2023**, *4*, 687–702. [[CrossRef](#)]
8. Piña-Ochoa, E.; Álvarez-Cobelas, M. Denitrification in Aquatic Environments: A Cross-System Analysis. *Biogeochemistry* **2006**, *81*, 111–130. [[CrossRef](#)]
9. Birgand, F.; Skaggs, R.W.; Chescheir, G.M.; Gilliam, J.W. Nitrogen Removal in Streams of Agricultural Catchments—A Literature Review. *Crit. Rev. Environ. Sci. Technol.* **2007**, *37*, 381–487. [[CrossRef](#)]
10. Zhao, S.; Zhang, B.; Sun, X.; Yang, L. Hot Spots and Hot Moments of Nitrogen Removal from Hyporheic and Riparian Zones: A Review. *Sci. Total Environ.* **2021**, *762*, 144168. [[CrossRef](#)]
11. Knowles, R. Denitrification. *Microbiol. Rev.* **1982**, *46*, 43–70. [[CrossRef](#)]
12. Seitzinger, S.; Harrison, J.A.; Böhlke, J.K.; Bouwman, A.F.; Lowrance, R.; Peterson, B.; Tobias, C.; Drecht, G.V. Denitrification across landscapes and waterscapes: A synthesis. *Ecol. Appl.* **2006**, *16*, 2064–2090. [[CrossRef](#)] [[PubMed](#)]
13. Wallenstein, M.D.; Myrold, D.D.; Firestone, M.; Voytek, M. Environmental controls on denitrifying communities and denitrification rates: Insights from molecular methods. *Ecol. Appl.* **2006**, *16*, 2143–2152. [[CrossRef](#)] [[PubMed](#)]
14. Silvennoinen, H.; Liikanen, A.; Torssonen, J.; Stange, C.F.; Martikainen, P.J. Denitrification and N₂O Effluxes in the Bothnian Bay (Northern Baltic Sea) River Sediments as Affected by Temperature under Different Oxygen Concentrations. *Biogeochemistry* **2008**, *88*, 63–72. [[CrossRef](#)]
15. Jickells, T.D.; Weston, K. Nitrogen Cycle—External Cycling. In *Treatise on Estuarine and Coastal Science*; Elsevier: Amsterdam, The Netherlands, 2011; pp. 261–278, ISBN 978-0-08-087885-0.
16. Lu, C.; Zhang, J.; Tian, H.; Crumpton, W.G.; Helmers, M.J.; Cai, W.-J.; Hopkinson, C.S.; Lohrenz, S.E. Increased Extreme Precipitation Challenges Nitrogen Load Management to the Gulf of Mexico. *Commun. Earth Environ.* **2020**, *1*, 21. [[CrossRef](#)]
17. Soana, E.; Gervasio, M.P.; Granata, T.; Colombo, D.; Castaldelli, G. Climate Change Impacts on Eutrophication in the Po River (Italy): Temperature-Mediated Reduction in Nitrogen Export but No Effect on Phosphorus. *J. Environ. Sci.* **2024**, *143*, 148–163. [[CrossRef](#)]
18. Gervasio, M.P.; Soana, E.; Granata, T.; Colombo, D.; Castaldelli, G. An Unexpected Negative Feedback between Climate Change and Eutrophication: Higher Temperatures Increase Denitrification and Buffer Nitrogen Loads in the Po River (Northern Italy). *Environ. Res. Lett.* **2022**, *17*, 084031. [[CrossRef](#)]
19. Pavan, V.; Antolini, G.; Barbiero, R.; Berni, N.; Brunier, F.; Cacciamani, C.; Cagnati, A.; Cazzuli, O.; Cicogna, A.; De Luigi, C.; et al. High Resolution Climate Precipitation Analysis for North-Central Italy, 1961–2015. *Clim. Dyn.* **2019**, *52*, 3435–3453. [[CrossRef](#)]
20. Persiano, S.; Ferri, E.; Antolini, G.; Domeneghetti, A.; Pavan, V.; Castellarin, A. Changes in Seasonality and Magnitude of Sub-Daily Rainfall Extremes in Emilia-Romagna (Italy) and Potential Influence on Regional Rainfall Frequency Estimation. *J. Hydrol. Reg. Stud.* **2020**, *32*, 100751. [[CrossRef](#)]
21. Soana, E.; Bartoli, M.; Milardi, M.; Fano, E.A.; Castaldelli, G. An Ounce of Prevention Is Worth a Pound of Cure: Managing Macrophytes for Nitrate Mitigation in Irrigated Agricultural Watersheds. *Sci. Total Environ.* **2019**, *647*, 301–312. [[CrossRef](#)]
22. Ludwig, W.; Dumont, E.; Meybeck, M.; Heussner, S. River Discharges of Water and Nutrients to the Mediterranean and Black Sea: Major Drivers for Ecosystem Changes during Past and Future Decades? *Prog. Oceanogr.* **2009**, *80*, 199–217. [[CrossRef](#)]
23. Blaas, H.; Kroeze, C. Excessive Nitrogen and Phosphorus in European Rivers: 2000–2050. *Ecol. Indic.* **2016**, *67*, 328–337. [[CrossRef](#)]
24. Grilli, F.; Accoroni, S.; Acri, F.; Bernardi Aubry, F.; Bergami, C.; Cabrini, M.; Campanelli, A.; Giani, M.; Guicciardi, S.; Marini, M.; et al. Seasonal and Interannual Trends of Oceanographic Parameters over 40 Years in the Northern Adriatic Sea in Relation to Nutrient Loadings Using the EMODnet Chemistry Data Portal. *Water* **2020**, *12*, 2280. [[CrossRef](#)]
25. Montanari, A.; Nguyen, H.; Rubineti, S.; Ceola, S.; Galelli, S.; Rubino, A.; Zanchettin, D. Why the 2022 Po River Drought Is the Worst in the Past Two Centuries. *Sci. Adv.* **2023**, *9*, eadg8304. [[CrossRef](#)]
26. Bonaldo, D.; Bellafiore, D.; Ferrarin, C.; Ferretti, R.; Ricchi, A.; Sangelantoni, L.; Vitelletti, M.L. The Summer 2022 Drought: A Taste of Future Climate for the Po Valley (Italy)? *Reg. Environ. Chang.* **2023**, *23*, 1. [[CrossRef](#)]
27. Gervasio, M.P.; Soana, E.; Vincenzi, F.; Magri, M.; Castaldelli, G. Drought-Induced Salinity Intrusion Affects Nitrogen Removal in a Deltaic Ecosystem (Po River Delta, Northern Italy). *Water* **2023**, *15*, 2405. [[CrossRef](#)]
28. Gervasio, M.P.; Soana, E.; Gavioli, A.; Vincenzi, F.; Castaldelli, G. Contrasting Effects of Climate Change on Denitrification and Nitrogen Load Reduction in the Po River (Northern Italy). *Environ. Sci. Pollut. Res.* **2024**, *31*, 48189–48204. [[CrossRef](#)]
29. Vezzoli, R.; Mercogliano, P.; Pecora, S.; Zollo, A.L.; Cacciamani, C. Hydrological Simulation of Po River (North Italy) Discharge under Climate Change Scenarios Using the RCM COSMO-CLM. *Sci. Total Environ.* **2015**, *521–522*, 346–358. [[CrossRef](#)]
30. Dalsgaard, T.; Nielsen, L.P.; Brotas, V.; Viaroli, P.; Underwood, G.; Nedwell, D.; Sundback, K.; Rysgaard, S.; Miles, A.; Bartoli, M.; et al. *Protocol Handbook for NICE-Nitrogen Cycling in Estuaries: A Project under the EU Research Programme: Marine Science and Technology (MAST III)*; Ministry of Environment and Energy National Environmental Research Institute: Silkeborg, Denmark; Department of Lake and Estuarine Ecology: Silkeborg, Denmark, 2000; pp. 1–62.
31. Owens, M.S.; Cornwell, J.C. The Benthic Exchange of O₂, N₂ and Dissolved Nutrients Using Small Core Incubations. *J. Vis. Exp.* **2016**, *104*, 54098. [[CrossRef](#)]
32. Braga, F.; Zaggia, L.; Bellafiore, D.; Bresciani, M.; Giardino, C.; Lorenzetti, G.; Maicu, F.; Manzo, C.; Riminucci, F.; Ravaioli, M.; et al. Mapping Turbidity Patterns in the Po River Prodelta Using Multi-Temporal Landsat 8 Imagery. *Estuar. Coast. Shelf Sci.* **2017**, *198*, 555–567. [[CrossRef](#)]

33. Nielsen, L.P. Denitrification in Sediment Determined from Nitrogen Isotope Pairing. *FEMS Microbiol. Lett.* **1992**, *86*, 357–362. [[CrossRef](#)]
34. Boldrin, A.; Langone, L.; Miserocchi, S.; Turchetto, M.; Aciri, F. Po River Plume on the Adriatic Continental Shelf: Dispersion and Sedimentation of Dissolved and Suspended Matter during Different River Discharge Rates. *Mar. Geol.* **2005**, *222–223*, 135–158. [[CrossRef](#)]
35. Menicucci, S.; De Felice, A.; Biagiotti, I.; Canduci, G.; Costantini, I.; Palermino, A.; Centurelli, M.; Leonori, I. Interannual Variation in the Zooplankton Community of the North Adriatic Sea under Short-Term Climatic Anomalies. *Diversity* **2024**, *16*, 291. [[CrossRef](#)]
36. Armstrong, F.A.J.; Stearns, C.R.; Strickland, J.D.H. The Measurement of Upwelling and Subsequent Biological Process by Means of the Technicon Autoanalyzer[®] and Associated Equipment. *Deep. Sea Res. Oceanogr. Abstr.* **1967**, *14*, 381–389. [[CrossRef](#)]
37. Kana, T.M.; Darkangelo, C.; Hunt, M.D.; Oldham, J.B.; Bennett, G.E.; Cornwell, J.C. Membrane Inlet Mass Spectrometer for Rapid High-Precision Determination of N₂, O₂, and Ar in Environmental Water Samples. *Anal. Chem.* **1994**, *66*, 4166–4170. [[CrossRef](#)]
38. Robertson, E.K.; Bartoli, M.; Brüchert, V.; Dalsgaard, T.; Hall, P.O.J.; Hellemann, D.; Hietanen, S.; Zilius, M.; Conley, D.J. Application of the Isotope Pairing Technique in Sediments: Use, Challenges, and New Directions. *Limnol. Ocean Methods* **2019**, *17*, 112–136. [[CrossRef](#)]
39. Steingruber, S.M.; Friedrich, J.; Gächter, R.; Wehrli, B. Measurement of Denitrification in Sediments with the ¹⁵N Isotope Pairing Technique. *Appl. Environ. Microbiol.* **2001**, *67*, 3771–3778. [[CrossRef](#)]
40. Eyre, B.D.; Rysgaard, S.; Dalsgaard, T.; Christensen, P.B. Comparison of Isotope Pairing and N₂:Ar Methods for Measuring Sediment Denitrification—Assumption, Modifications, and Implications. *Estuaries* **2002**, *25*, 1077–1087. [[CrossRef](#)]
41. Pinheiro, J.; Bates, D.; DebRoy, S.; Sarkar, D.; R Core Team. nlme: Linear and Nonlinear Mixed Effects Models. *R Package Version* **2018**, *3*, 1–137.
42. Deichmann, U.; Schuster, S.; Mazat, J.; Cornish-Bowden, A. Commemorating the 1913 Michaelis–Menten Paper Die Kinetik Der Invertinwirkung: Three Perspectives. *FEBS J.* **2014**, *281*, 435–463. [[CrossRef](#)]
43. De Klein, J.J.M.; Overbeek, C.C.; Juncher Jørgensen, C.; Veraart, A.J. Effect of Temperature on Oxygen Profiles and Denitrification Rates in Freshwater Sediments. *Wetlands* **2017**, *37*, 975–983. [[CrossRef](#)]
44. Johnson, M.F.; Albertson, L.K.; Algar, A.C.; Dugdale, S.J.; Edwards, P.; England, J.; Gibbins, C.; Kazama, S.; Komori, D.; MacColl, A.D.C.; et al. Rising Water Temperature in Rivers: Ecological Impacts and Future Resilience. *WIREs Water* **2024**, *11*, e1724. [[CrossRef](#)]
45. Perkins, D.M.; Yvon-Durocher, G.; Demars, B.O.L.; Reiss, J.; Pichler, D.E.; Friberg, N.; Trimmer, M.; Woodward, G. Consistent Temperature Dependence of Respiration across Ecosystems Contrasting in Thermal History. *Glob. Chang. Biol.* **2012**, *18*, 1300–1311. [[CrossRef](#)]
46. Saunders, D.L.; Kalff, J. Nitrogen Retention in Wetlands, Lakes and Rivers. *Hydrobiologia* **2001**, *443*, 205–212. [[CrossRef](#)]
47. Boulêtreau, S.; Lyautey, E.; Dubois, S.; Compin, A.; Delattre, C.; Touron-Bodilis, A.; Mastrorillo, S.; Garabetian, F. Warming-Induced Changes in Denitrifier Community Structure Modulate the Ability of Phototrophic River Biofilms to Denitrify. *Sci. Total Environ.* **2014**, *466–467*, 856–863. [[CrossRef](#)] [[PubMed](#)]
48. Velthuis, M.; Veraart, A.J. Temperature Sensitivity of Freshwater Denitrification and N₂O Emission—A Meta-Analysis. *Glob. Biogeochem. Cycles* **2022**, *36*, e2022GB007339. [[CrossRef](#)]
49. Speir, S.L.; Tank, J.L.; Taylor, J.M.; Grose, A.L. Temperature and Carbon Availability Interact to Enhance Nitrous Oxide Production via Denitrification in Alluvial Plain River Sediments. *Biogeochemistry* **2023**, *165*, 191–203. [[CrossRef](#)]
50. Veraart, A.J.; De Klein, J.J.M.; Scheffer, M. Warming Can Boost Denitrification Disproportionately Due to Altered Oxygen Dynamics. *PLoS ONE* **2011**, *6*, e18508. [[CrossRef](#)]
51. Ward, B.B. Nitrification: An Introduction and Overview of the State of the Field. In *Nitrification*; Ward, B.B., Arp, D.J., Klotz, M.G., Eds.; ASM Press: Washington, DC, USA, 2014; pp. 1–8, ISBN 978-1-68367-116-9.
52. Qu, W.; Suo, L.; Liu, R.; Liu, M.; Zhao, Y.; Xia, L.; Fan, Y.; Zhang, Q.; Gao, Z. Influence of Temperature on Denitrification and Microbial Community Structure and Diversity: A Laboratory Study on Nitrate Removal from Groundwater. *Water* **2022**, *14*, 436. [[CrossRef](#)]
53. Brin, L.D.; Giblin, A.E.; Rich, J.J. Similar Temperature Responses Suggest Future Climate Warming Will Not Alter Partitioning between Denitrification and Anammox in Temperate Marine Sediments. *Glob. Chang. Biol.* **2017**, *23*, 331–340. [[CrossRef](#)]
54. Verstraete, W.; Forcht, D.D. Biochemical Ecology of Nitrification and Denitrification [Soils]. In *Advances in Microbial Ecology*; Springer: Boston, MA, USA, 1977; pp. 135–214.
55. Nogaro, G.; Burgin, A.J. Influence of Bioturbation on Denitrification and Dissimilatory Nitrate Reduction to Ammonium (DNRA) in Freshwater Sediments. *Biogeochemistry* **2014**, *120*, 279–294. [[CrossRef](#)]
56. Racchetti, E.; Bartoli, M.; Soana, E.; Longhi, D.; Christian, R.R.; Pinaridi, M.; Viaroli, P. Influence of Hydrological Connectivity of Riverine Wetlands on Nitrogen Removal via Denitrification. *Biogeochemistry* **2011**, *103*, 335–354. [[CrossRef](#)]
57. Inwood, S.E.; Tank, J.L.; Bernot, M.J. Factors Controlling Sediment Denitrification in Midwestern Streams of Varying Land Use. *Microb. Ecol.* **2007**, *53*, 247–258. [[CrossRef](#)] [[PubMed](#)]
58. Soana, E.; Naldi, M.; Bonaglia, S.; Racchetti, E.; Castaldelli, G.; Brüchert, V.; Viaroli, P.; Bartoli, M. Benthic Nitrogen Metabolism in a Macrophyte Meadow (*Vallisneria spiralis* L.) under Increasing Sedimentary Organic Matter Loads. *Biogeochemistry* **2015**, *124*, 387–404. [[CrossRef](#)]

59. Tesi, T.; Miserocchi, S.; Acri, F.; Langone, L.; Boldrin, A.; Hatten, J.A.; Albertazzi, S. Flood-Driven Transport of Sediment, Particulate Organic Matter, and Nutrients from the Po River Watershed to the Mediterranean Sea. *J. Hydrol.* **2013**, *498*, 144–152. [[CrossRef](#)]
60. Stelzer, R.S.; Thad Scott, J.; Bartsch, L.A.; Parr, T.B. Particulate Organic Matter Quality Influences Nitrate Retention and Denitrification in Stream Sediments: Evidence from a Carbon Burial Experiment. *Biogeochemistry* **2014**, *119*, 387–402. [[CrossRef](#)]
61. Seitzinger, S. Linkages between Organic Matter Mineralization and Denitrification in Eight Riparian Wetlands. *Biogeochemistry* **1994**, *25*, 19–39. [[CrossRef](#)]

Disclaimer/Publisher’s Note: The statements, opinions and data contained in all publications are solely those of the individual author(s) and contributor(s) and not of MDPI and/or the editor(s). MDPI and/or the editor(s) disclaim responsibility for any injury to people or property resulting from any ideas, methods, instructions or products referred to in the content.